



University of  
Zurich<sup>UZH</sup>

Zurich Open Repository and  
Archive

University of Zurich  
University Library  
Strickhofstrasse 39  
CH-8057 Zurich  
[www.zora.uzh.ch](http://www.zora.uzh.ch)

---

Year: 2024

---

## Corrin Ring Modifications Reveal the Chemical and Spatial Requirements for the B<sub>12</sub> *btuB* Riboswitch Interaction

Musiari, Anastasia ; Reichenbach, María ; Gallo, Sofia ; Sigel, Roland K O

DOI: <https://doi.org/10.1002/chem.202401800>

Posted at the Zurich Open Repository and Archive, University of Zurich

ZORA URL: <https://doi.org/10.5167/uzh-262814>

Journal Article

Published Version



The following work is licensed under a Creative Commons: Attribution-NonCommercial-NoDerivatives 4.0 International (CC BY-NC-ND 4.0) License.

Originally published at:

Musiari, Anastasia; Reichenbach, María; Gallo, Sofia; Sigel, Roland K O (2024). Corrin Ring Modifications Reveal the Chemical and Spatial Requirements for the B<sub>12</sub> *btuB* Riboswitch Interaction. *Chemistry*, 30(49):e202401800. DOI: <https://doi.org/10.1002/chem.202401800>

# Corrin Ring Modifications Reveal the Chemical and Spatial Requirements for the B<sub>12</sub>-*btuB* Riboswitch Interaction

Anastasia Musiari,<sup>[a]</sup> María Reichenbach,<sup>[a]</sup> Sofia Gallo,<sup>\*,[a]</sup> and Roland K. O. Sigel<sup>\*,[a]</sup>

Dedicated to Prof. Dr. Roger Alberto on the occasion of his 65<sup>th</sup> birthday with the very best wishes of the authors.

The *btuB* riboswitch is a regulatory RNA sequence controlling gene expression of the outer membrane B<sub>12</sub> transport protein BtuB by specifically binding coenzyme B<sub>12</sub> (AdoCbl) as its natural ligand. The B<sub>12</sub> sensing riboswitch class is known to accept various B<sub>12</sub> derivatives, leading to a division into two riboswitch subclasses, dependent on the size of the apical ligand. Here we focus on the role of side chains *b* and *e* on affinity and proper recognition, i.e. correct structural switch of the *btuB* RNA, which belongs to the AdoCbl-binding class I.

Chemical modification of these side chains disturbs crucial hydrogen bonds and/or electrostatic interactions with the RNA, its effect on both affinity and switching being monitored by in-line probing. Chemical modifications at sidechain *b* of vitamin B<sub>12</sub> show larger effects indicating crucial B<sub>12</sub>-RNA interactions. When introducing the same modification to AdoCbl the influence of any side-chain modification tested is reduced. This renders the impact of the adenosyl-ligand for B<sub>12</sub>-*btuB* riboswitch recognition clearly beyond the known role in affinity.

## Introduction

Gene regulation involving a riboswitch is based on the recognition of a specific cellular metabolite by a conserved but untranslated part of a mRNA sequence, i.e. the riboswitch.<sup>[1,2]</sup> Typically found in bacteria, riboswitches are composed of two domains: First, the aptamer domain, which is highly conserved in sequence and structure, and which comprises the binding core for the metabolite. Second, the functional domain called expression platform, where structural changes occurring from ligand binding are transduced, leading to gene regulation at both transcriptional and/or translational level.<sup>[3,4]</sup>

B<sub>12</sub>-sensing riboswitches, also called Cbl riboswitches, are a widespread riboswitch class including also the *btuB* riboswitch of *E. coli* used in this study.<sup>[1]</sup> These riboswitches specifically recognize some of the largest and most complex cellular metabolites, cobalamins (Figure 1A). Cbl riboswitches are thus mainly involved in the gene regulation of enzymes involved in cobalamin synthesis, but are also found to regulate the synthesis of porphyrins and the expression of cobalamin transporters.<sup>[5]</sup> For example, the *btuB* riboswitch controls the gene expression of the outer membrane receptor protein BtuB,

which is responsible for the active transport of cobalamins into the periplasmic space.<sup>[4,6]</sup>

In contrast to other riboswitch classes<sup>[7]</sup> Cbl riboswitches have a broad spectrum of selectivity towards different corrinoids, which was shown in several studies with natural and synthetic B<sub>12</sub>-derivatives.<sup>[8–11,12]</sup> In 2012 the first X-ray structures of Cbl riboswitches were published by Batey<sup>[13]</sup> and Serganov,<sup>[14]</sup> providing new molecular insights into the molecular structure of this riboswitch class and the binding principles to their respective B<sub>12</sub> ligand (Figure 1B and C). A further internal classification was thereafter established classifying representatives preferentially binding to Coenzyme B<sub>12</sub> (AdoCbl) as class I Cbl riboswitches, and those specific for cobalamins with smaller apical ligands such as methylcobalamin (MeCbl) and aquocobalamin (AqCbl) as class II Cbl riboswitches.<sup>[13]</sup> It was demonstrated that the classification into class I or class II was related to the presence or absence of a large aptameric domain encompassing P7-P11 (Figure 1D).<sup>[11]</sup> The *btuB* riboswitch of *E. coli* belongs to the AdoCbl-binding class I, as supported by previous investigations.<sup>[1,4,8]</sup> Although this riboswitch can interact also with vitamin B<sub>12</sub> (CNCbl) and other B<sub>12</sub>-derivatives, binding occurs with distinctly lower affinity and/or incomplete reorganisation depending on the degree of derivatization of the B<sub>12</sub>.<sup>[1,8,15]</sup>

Some understanding for a correct or disadvantageous interaction respectively can be gained from the five structures of Cbl-riboswitches solved to date.<sup>[10,13,14]</sup> The crystal structures indicate that van der Waals surface complementarity between cobalamin and the RNA binding pocket is an important driving force for the interaction,<sup>[13,14]</sup> as implicated by the adenosyl moiety on the β-side (Figure 1E) inserted into a highly specific riboswitch cavity. The seven protruding amide sidechains of the corrin ring are predestined to be involved in a large hydrogen bonding network with the bases and the backbone of surrounding nucleotides. However, the crystal structures show

[a] A. Musiari, M. Reichenbach, S. Gallo, R. K. O. Sigel  
Department of Chemistry, University of Zurich, Winterthurerstrasse 190,  
CH-8057 Zurich, Switzerland  
E-mail: roland.sigel@chem.uzh.ch  
sofia.gallo@chem.uzh.ch

Supporting information for this article is available on the WWW under  
<https://doi.org/10.1002/chem.202401800>

© 2024 The Authors. Chemistry - A European Journal published by Wiley-VCH GmbH. This is an open access article under the terms of the Creative Commons Attribution Non-Commercial NoDerivs License, which permits use and distribution in any medium, provided the original work is properly cited, the use is non-commercial and no modifications or adaptations are made.

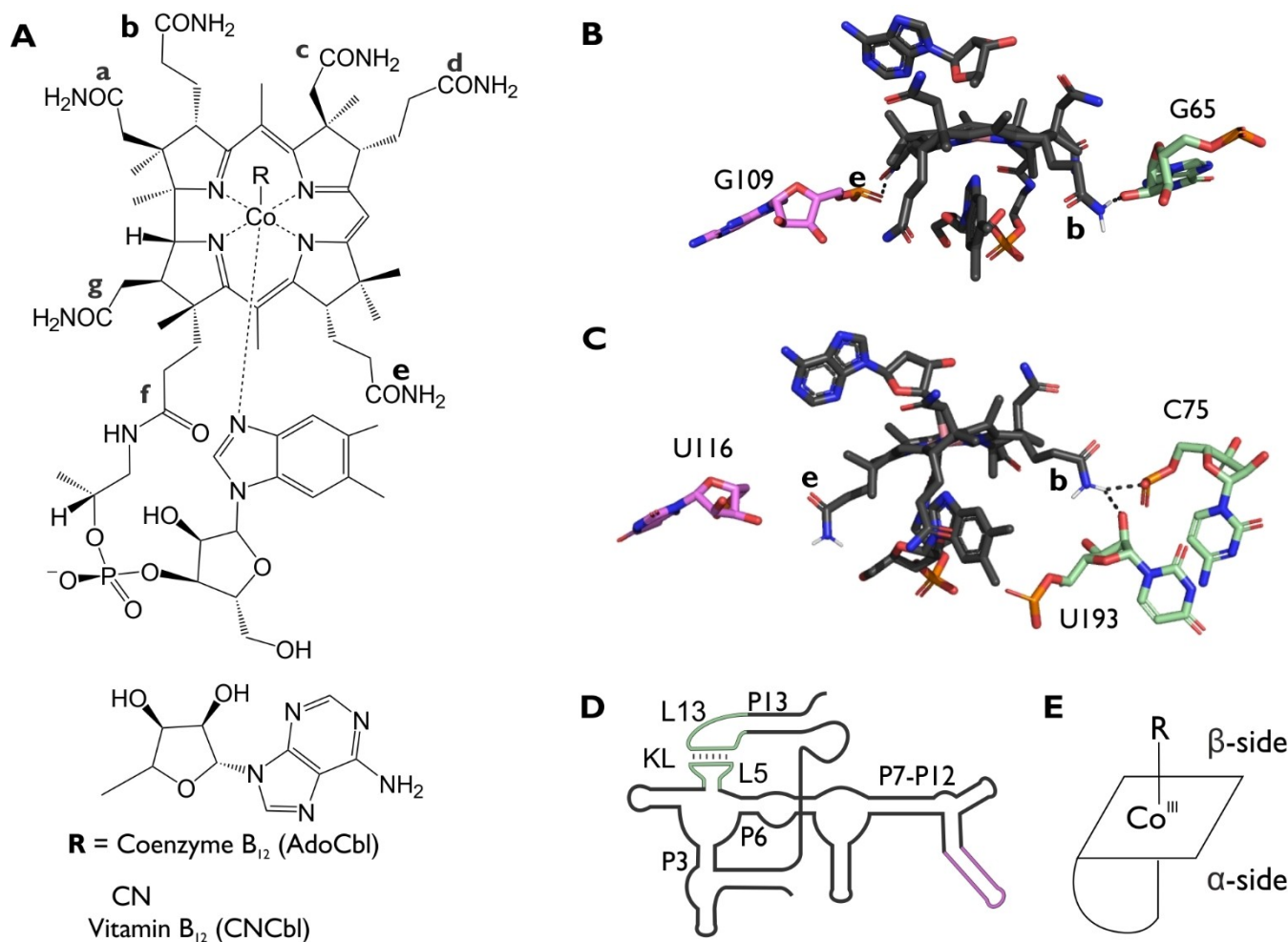


**Figure 1.** A Chemical structure of coenzyme B<sub>12</sub> and vitamin B<sub>12</sub> lettering the seven amides at the corrin ring. **B** Section of the crystal structure of the bound coenzyme B<sub>12</sub> to the riboswitch from *Symbiobacterium thermophilum* (*Sth* riboswitch, PDB 4GXV) emphasizing the hydrogen bonds of sidechains *b* and *e*. **C** Corresponding section from the *Thermoanaerobacter tengcongensis* riboswitch (*Tte* riboswitch, PDB 4GMA) with the hydrogen bond at sidechain *e* missing. The nucleotides in close proximity to the metabolite are marked according to the color coding in **D**. **D** Schematic representation of the *btuB* riboswitch indicating the position of the kissing loop (KL, light green) interaction between loops 5 and 13 (L5, L13) and the P11 stem (pink). **E** Definition of the  $\alpha$ -side (lower) and the  $\beta$ -side (upper) of Cbl compounds.

this network only to be partially exploited. Interaction to the riboswitch is mainly mediated by the  $\beta$ -sidechains *a* and *c*, in line with previous observations in solution that sidechain *c* has a severe impact on the *btuB* riboswitch fold.<sup>[15]</sup> The involvement in H-bonding of the third  $\beta$ -sidechain *g* is unclear and might be related to the formation of the L5-L13 kissing loop: While in both, the *Tte* riboswitch<sup>[13]</sup> and the *B.subtilis* B<sub>12</sub> riboswitch<sup>[10]</sup> this sidechain interacts with a nucleotide of P5, in the *Sth* riboswitch, which was crystallized without the downstream L/P13 region, no such interaction was seen.<sup>[14]</sup> The  $\alpha$ -side of the corrin ring similarly displays an abundance of possible hydrogen bond donor and acceptor sites, but again which are to a large part only partly exploited, and with sidechain *d* so far never found involved in binding. A recent study extensively investigated the *f*-sidechain revealing that the identity of the ligand is not directly noticed but rather the shape complementarity and the base-on or -off orientation.<sup>[9]</sup>

Here, we elucidate the role of the two  $\alpha$ -propanamide sidechains *b* and *e* (Figure 1A) for the cobalamin interaction to the *btuB* riboswitch. Sidechain *b* was previously found to be involved in hydrogen bonds with its amide to a riboswitch nucleotide in all structures, whereas sidechain *e* acts as hydrogen bond donor only in one structure.<sup>[13,14]</sup> In general, the information on the importance of these two side chains in recognition of and switching the RNA is very scarce. By applying in-line probing assays<sup>[16]</sup> with several cobalamin derivatives we followed the structural changes of the riboswitch at a single nucleotide resolution providing a picture not only on the general affinity but also on their ability to correctly induce the necessary change in the RNA three-dimensional fold.

## Results and Discussion

To investigate the importance of hydrogen bond capabilities of the *b*- and *e*-sidechains for riboswitch recognition and interaction, we synthesized and characterized six different B<sub>12</sub> derivatives: The two cyanocobalamin (CNCbl) derivatives ethyl *b*-amide CNCbl (1) and dimethyl *e*-amide CNCbl (2), as well as the AdoCbl derivatives ethyl *b*-amide AdoCbl (3), dimethyl *e*-amide AdoCbl (4), *b*-acid AdoCbl (5), and *e*-acid AdoCbl (6) (Figure 2). The chemical modifications at either of the two sidechains from an originally primary amide to a secondary (compounds 1,3) or tertiary amide (compounds 2,4) with hydrophobic alkyl groups alter the H-bonding ability towards the riboswitch. Substitution of one proton by a single ethyl-group (1 and 3) still allows the formation of one hydrogen bond. Compounds 2 and 4 lack any donor properties, and thus strong binding alterations are expected should sidechain *e* be involved in a crucial interaction with the B<sub>12</sub>-riboswitch.

The *btuB* riboswitch belongs to the AdoCbl-binding subclass I, but it still correctly recognizes vitamin B<sub>12</sub>, although with a reduced affinity.<sup>[6]</sup> By including both the AdoCbl as well as the CNCbl derivatives, we can clearly differentiate affinity from purely structural effects. In a previous study,<sup>[15]</sup> we had

determined that the *b*- and *e*- acid CNCbl derivatives display a decreased affinity towards the *btuB* riboswitch. As it is unclear if this effect was caused by the sidechain modification or the cyano ligand, we here include also the AdoCbl-acid derivatives *b*-acid AdoCbl (5) and *e*-acid AdoCbl (6). All derivatives alter the hydrogen bonding properties, and the two acid derivatives additionally introduce a negative charge at physiological pH. Interaction of all compounds 1–6 was monitored by in-line probing<sup>[15,16]</sup> to investigate the influence of these punctual chemical modifications on the RNA structure on an atomic level.

Syntheses of the B<sub>12</sub> Derivatives

Ethyl *b*-amide CNCbl (1) was synthesized with an overall yield of 34% from *b*-acid CNCbl<sup>[17,18]</sup> in the presence of ethylamine hydrochloride and using EDAC hydrochloride as a catalyst in analogy to similar reactions described in the literature<sup>[19]</sup> (Figure 2B). The reaction was monitored by HPLC (Figure S.8). After 24 h most of the starting material was converted to the final product and an intermediate formed by the adduct between the *b*-acid CNCbl and EDAC. Full conversion into the final

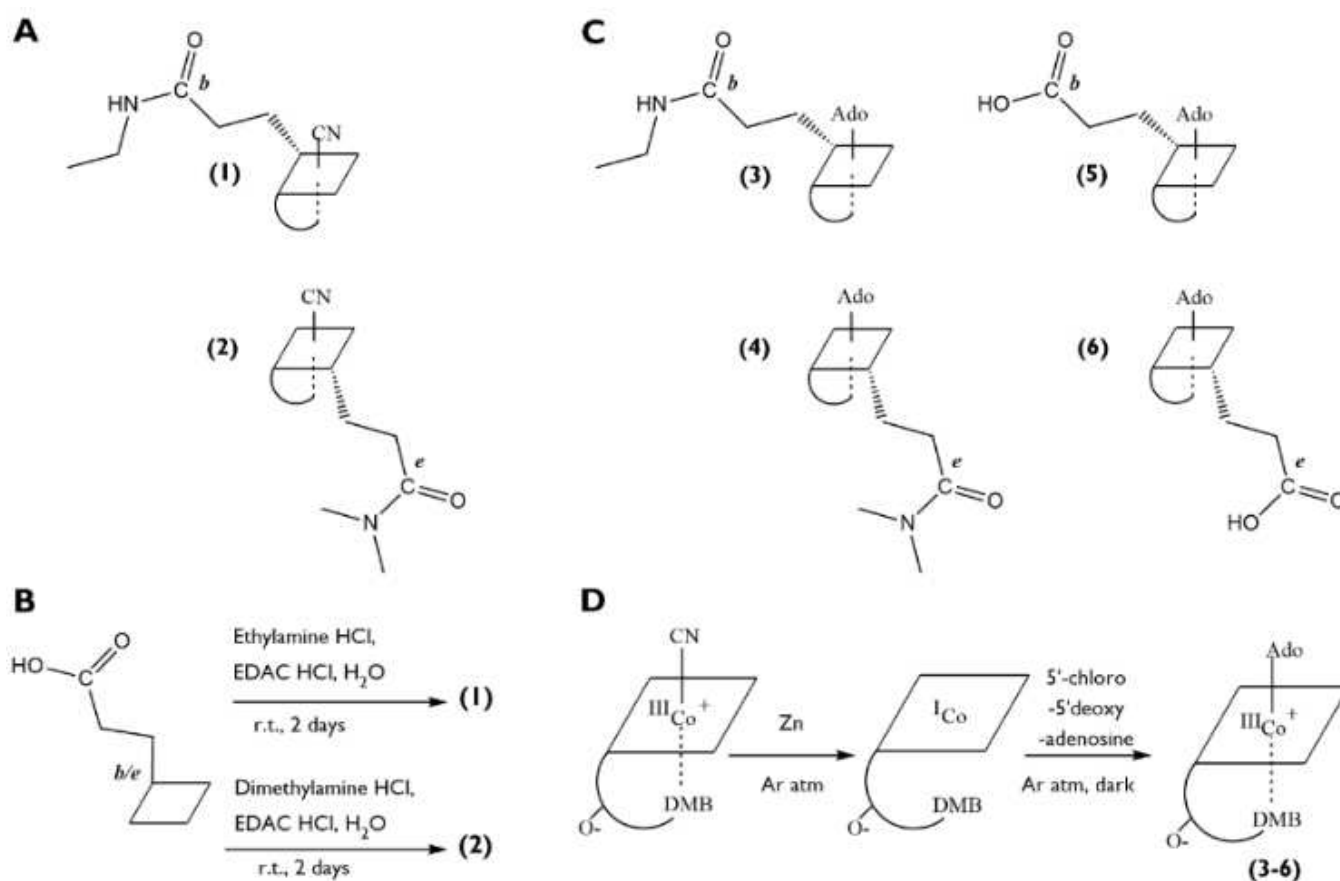


**Figure 2.** Schematic representation of the Cbl derivatives studied in this work including their synthesis scheme. **A** The two vitamin B<sub>12</sub> derivatives tested are *b*-ethylamine-CNCbl (1) and *e*-dimethylamine-CNCbl (2). **B** Synthetic scheme of the reaction conditions to prepare the amide derivatives. **C** The four tested coenzyme B<sub>12</sub> derivatives are *b*-ethylamine-AdoCbl (3), *b*-acid-AdoCbl (4), *e*-dimethylamine-AdoCbl (5) and *e*-acid-AdoCbl (6). **D** Synthetic scheme of the reaction conditions to convert the vitamin B<sub>12</sub> derivatives into coenzyme derivatives.

product (1) could not be achieved, neither by increasing the reaction time nor by increasing the temperature. The formation and stability of this intermediate together with the close HPLC retention time to the product (1) lead to a rather small yield. The identity of product (1) was confirmed by ESI-MS and NMR. The ESI-spectrum shows a peak at  $m/z = 1383.7$  corresponding to the mass of the protonated product (1) and one at  $m/z = 692.6$  corresponding to the doubly charged product.  $^{13}\text{C}$ -NMR and  $^1\text{H}$ -NMR characterization was done by an  $[\text{}^1\text{H},^{13}\text{C}]$ -HSQC experiment and comparison with spectra of other  $\text{B}_{12}$ -derivatives.<sup>[8,20–23]</sup> The  $^1\text{H}$ -NMR spectrum of ethyl *b*-amide CNCbl (1) (Figure S.2) shows the appearance of two multiplets corresponding to the ethyl group of the *b*-sidechain, a quartet at 3.12 ppm ( $\text{H}_2\text{-C33et1}$ ) and a respective triplet at 1.04 ppm ( $\text{H}_3\text{-C33et2}$ ). In comparison to Vitamin  $\text{B}_{12}$ , the  $[\text{}^1\text{H},^{13}\text{C}]$ -HSQC spectra of (1) shows additional resonances at 34.53 ppm and 13.53 ppm corresponding to C33et1 and C33et2 respectively (Figure S.3). In spite of the overlay with the signal of C132, C33et1 was unambiguously assigned due to its crosscorrelation to the signal at 3.27 ppm in the  $^1\text{H}$ -NMR spectrum. As a consequence of alkylation, also the signals of the two *b*-sidechain carbons, C31 and C32, are downfield shifted in comparison with Vitamin  $\text{B}_{12}$ .

**Dimethyl *e*-amide CNCbl (2)** was synthesized with an overall yield of 29% from *e*-acid CNCbl<sup>[17,18]</sup> in the presence of dimethylamine hydrochloride and EDAC hydrochloride as a catalyst in analogy to 1 and with similar compounds in the literature<sup>[19]</sup> (Figure 2B). The reaction was monitored by HPLC (Figure S.9). After 3 hours the starting material was already partially converted to the product and to the intermediate formed by the adduct between the *e*-acid CNCbl and EDAC. After two days the starting material was mostly consumed, however the intermediary adduct proved again very stable hampering the yield. The identity of product (2) was confirmed by ESI-MS and NMR. The ESI-spectrum of dimethyl *e*-amide CNCbl shows a peak at  $m/z = 1383.7$  corresponding to the mass of the protonated product (2) and one at  $m/z = 692.5$  corresponding to the doubly charged product. As for (1)  $^{13}\text{C}$ -NMR and  $^1\text{H}$ -NMR characterization of (2) was facilitated by an additional  $[\text{}^1\text{H},^{13}\text{C}]$ -HSQC experiment and by comparison with NMR-spectra of other  $\text{B}_{12}$ -derivatives.<sup>[8,20,21]</sup> The  $^1\text{H}$ -NMR spectrum of dimethyl *e*-amide CNCbl (Figure S.4) shows the appearance of two new resonances corresponding to the two methyl substituents introduced in the *e*-sidechain, one singlet at 3.09 ppm ( $\text{H}_2\text{-C133dimeA}$ ) and a second at 2.93 ppm ( $\text{H}_3\text{-C133dimeB}$ ), which could be unambiguously assigned due to their crosscorrelation to the signals at 37.93 ppm and 35.53 ppm in the  $^{13}\text{C}$ -NMR spectrum. Due to the modification, also the resonances of the *e*-sidechain carbons shifted downfield in comparison to Vitamin  $\text{B}_{12}$  as shown for C131 in Figure S.5.

**Ethyl *b*-amide AdoCbl (3), dimethyl *e*-amide AdoCbl (4), *b*-acid AdoCbl (5) and *e*-acid AdoCbl (6)** are AdoCbl derivatives and were all synthesised from their corresponding CNCbl derivative, ethyl *b*-amide CNCbl (1), dimethyl *e*-amide CNCbl (2), *b*-acid CNCbl and *e*-acid CNCbl by replacing the cyanide apical ligand with an adenosyl group (Figure 2D) as described in the

literature for other CNCbl derivatives.<sup>[23]</sup> Products were obtained with overall yields of 20–35%. The reactions were monitored by HPLC where the formation of the adenylated product was typically observed already after one hour (see the trace of the raw product of (6) in Figure S.10 as a representative for all adenylation reactions). The reaction mixtures were purified by preparative HPLC and the identity of the respective product (3–6) was confirmed by UV-Vis (see the spectrum of (6) in Figure S.11 as a representative for all AdoCbl-derivatives (3–6)). While the UV-Vis spectra of CNCbl derivatives show a characteristic  $\gamma$  band at around 360 nm, the introduction of the adenosyl moiety leads to a strong decrease thereof and to the appearance of a new band at around 260 nm.<sup>[24]</sup> The ESI-spectra of all four adenylated products (3–6) show one peak at a  $m/z$  value corresponding to the mass of the protonated product  $[\text{M} + \text{H}]^+$ , one corresponding to the doubly charged product  $[\text{M} + 2\text{H}]^{2+}$  and one to the triply charged product  $[\text{M} + 3\text{H}]^{3+}$ .  $^{13}\text{C}$ -NMR and  $^1\text{H}$ -NMR characterization of (3–6) was facilitated by additional  $[\text{}^1\text{H},^{13}\text{C}]$ -HSQC experiments and by comparison with NMR-spectra of other  $\text{B}_{12}$ -derivatives<sup>[8,20,21]</sup> with the resonances of the adenosyl moiety being the most characteristic (see spectra of (6) in Figures S.6 and S.7 as representatives for all AdoCbl-derivatives (3–6)).

## Interaction Studies With the *btuB* Riboswitch

### *In-Line Probing Reveals Aberrations in RNA Refolding by Binding to the New Derivatives*

In-line probing allows to monitor structural changes of RNA and is a widely used technique to follow metabolite binding and subsequent induced structural changes of riboswitches.<sup>[16,25]</sup> This method exploits the inherent instability of RNA due to 2'-OH provoked self-cleavage of its backbone. This self-cleavage reaction very much depends on the so-called “in-line” positioning of the attacking hydroxyl-group and the 5'-oxygen of the consecutive nucleotide. The reaction is therefore very sensitive to the local structural environment of the RNA, and reorganization thereof can lead to either increasing or decreasing cleavage activity at specific sites.<sup>[25]</sup> Subsequent separation of the cleavage products by PAGE allows to visualize and quantify such changes.

The structural rearrangement of the *btuB* riboswitch from *E. coli* upon binding AdoCbl and other  $\text{B}_{12}$  derivatives has already been investigated by in-line probing in numerous works.<sup>[1,8,15]</sup> It was shown that the apical adenosyl moiety (on the  $\beta$ -side) is determinant for the affinity to the riboswitch, while the introduction of a carboxylate in one of the corrin ring sidechains b, c, d or e lead to an altered cleavage pattern.<sup>[8,15]</sup> It was thereby demonstrated that out of these four sidechains, the modification at sidechain e was the least deleterious for the rearrangement of the *btuB* riboswitch, while a carboxylate at sidechain c led to a completely altered switch.

The six  $\text{B}_{12}$  derivatives (1–6) were thus incubated with the *btuB* riboswitch and the influence of the chemical modifications in their interaction with the RNA monitored by in-line probing.



The RNA used for these experiments is a 5'-end radioactive labeled 216 nt long *btuB* riboswitch sequence comprising the 202 nt long aptamer region and short extensions at both ends, as it has been used previously (Figure 1D).<sup>[26]</sup> Cleavage sites were visualised by denaturing long PAGE to obtain a highest possible footprinting resolution. Intensity changes at ten specific cleavage sites (Figure 3) were monitored to provide

information regarding the completeness of the structural rearrangement of the *btuB* riboswitch upon binding to the respective derivative (1-6). This includes an additionally observed cleavage site located at G151 which was identified in all our experiments, but which was not described so-far. This so-called site 6b, is located in the junction J6/3 which plays a crucial role for ligand recognition.<sup>[27]</sup> Its cleavage intensity is

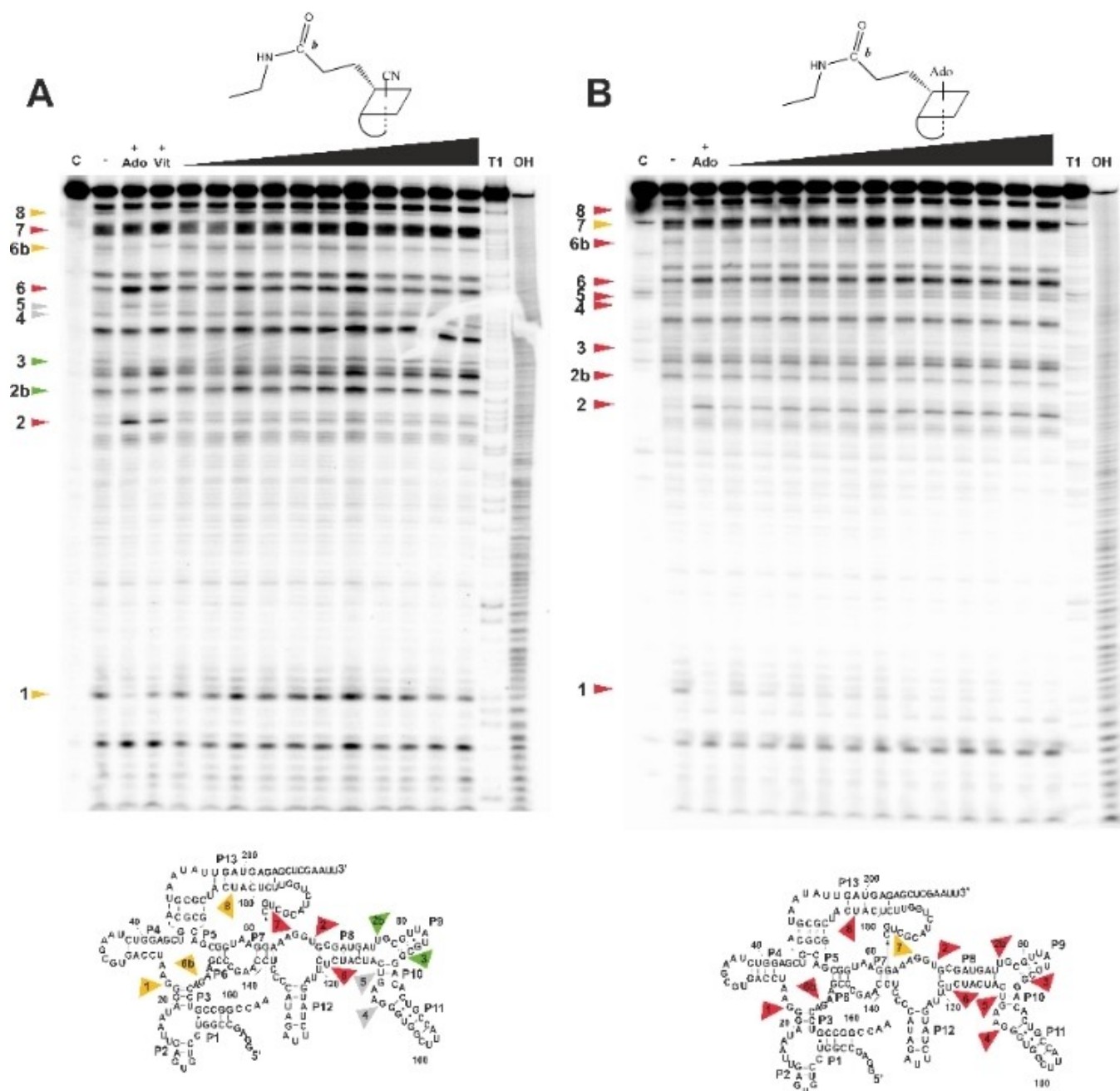


**Figure 3.** In-line probing experiments with the *btuB* riboswitch and ethyl *b*-amide CNCbl (1) as well as ethyl *b*-amide AdoCbl (3). The titration experiments with ethyl *b*-amide CNCbl (1) (A) and ethyl *b*-amide AdoCbl (3) (B) were performed using AdoCbl 10  $\mu$ M (+ Ado) and CNCbl 1 mM (+ Vit) as references. Lane “c” corresponds to the unreacted RNA, “-” to the RNA incubated without B<sub>12</sub>, “T1” to the RNase T1 digestion and “OH” to the alkaline digestion ladder. The arrows indicate the individual characteristic cleavage sites for the *btuB* riboswitch that show an intensity change in the presence of AdoCbl. Grey arrows indicate sites that do not change in intensity after addition of (1) and (3) respectively, green arrows indicate trends opposite to the one expected, red indicates expected cleavage and orange arrows indicate not quantifiable trends. The B<sub>12</sub> concentration range used for ethyl *b*-amide CNCbl was 5  $\mu$ M–2.5 mM, while for ethyl *b*-amide AdoCbl it was 50 nM–100  $\mu$ M. The trends found at the indicated sites are mapped onto the secondary riboswitch structure (shown below the respective gel).

decreasing in the presence of AdoCbl pointing to a lower flexibility of the RNA backbone at this site upon ligand binding.

A first overview experiment with the non-adenylated and adenylated amide derivatives (1–4) showed that all the applied derivatives can at least partially switch the *btuB* riboswitch (Figure S12). For most derivatives not all known cleavage bands are equally affected revealing that the inserted modifications prevent the riboswitch from complete and/or concerted reorganization. Furthermore, this first overview already shows that the AdoCbl derivatives have a much higher affinity towards the riboswitch than the CNCbl derivatives which is in line with earlier experiments. Therefore, B<sub>12</sub> concentration used in the subsequent titration experiments was adapted accordingly to 5 μM–2.5 mM for the CNCbl derivatives and of 50 nM–100 μM for the AdoCbl derivatives.

### ***Epecially Modifications at Sidechain b of VitB<sub>12</sub>-Derivates Have a Large Effect on the Structural Switch***

From the crystal structures it is known that the NH<sub>2</sub> group of the amide *b*-sidechain is involved in two hydrogen bonds.<sup>[13,14]</sup> In the case of the *Symbiobacterium thermophilum* (*Sth*) riboswitch, whose crystallized sequence misses the P13-extension, both hydrogen bonds are directed towards one single nucleotide of P5 (2'-OH and 3'-O). The second crystallized riboswitch from *Thermoanaerobacter tengcongensis* (*Tte*) also contains the P13-extension with a hydrogen bond towards the 2'-OH non-bridging phosphate oxygen. However the second hydrogen bonds of sidechain *b* is directed towards the corresponding nucleotide in the P5 region (non-bridging phosphate oxygen).<sup>[13,14]</sup> The *b*-sidechain is therefore determinant for stabilising the regulatory KL interaction between L5 and L13 and is most probably also crucial for the proper regulatory function.

The introduction of a secondary amide group as in compounds 1 and 3 is expected to partially abolish hydrogen bond formation<sup>[28]</sup> as only one N–H is still present. In addition, the newly introduced ethyl group varies the local hydrophobic features leading to alternative interaction and/or changes in affinity. The second here investigated modification at site *b* includes a carboxylate to give *b*-acid AdoCbl (5). At the characteristic in-line probing pH of 8.3 this newly introduced group is fully deprotonated and therefore not able to act as a hydrogen bond donor. In contrary, if involved in any interactions with the equally negatively charged RNA, it could act as a hydrogen bond acceptor possibly interacting with O–H groups of close by ribose moieties or coordinate to a metal ion.

In-line probing titration experiments showed that the presence of ethyl *b*-amide CNCbl (1) leads to an aberrant switch of the RNA with evaluable intensity changes at sites 2, 6 and 7 and slight intensity changes, which are visible but cannot be evaluated quantitatively, at sites 1, 6b and 8 (Figure 3A, sites marked in red and orange respectively). Intensity changes are also visible at sites 2b and 3 but with an opposite trend to the one expected, i.e. showing an increase of cleavage activity in contrast to the expected decrease (Figure S.3 A, sites marked in

green). Interestingly, these two sites and the two unaffected sites 4 and 5 are located in the P6-extension of the aptamer. This large peripheral RNA region is present in class I B<sub>12</sub>-riboswitches responding to AdoCbl but not in those of class II, which are regulated by so-called small cobalamines such as aquocobalamin and methylcobalamin.<sup>[13,14]</sup> Indeed, the P6-extension is essential for the formation of the highly specific adenosyl binding pocket. Since this divergence in the general in-line probing pattern was not observed by interaction with Vitamin B<sub>12</sub> itself, the prevention of a correct P6-rearrangement might, therefore, mainly result from the introduced side-chain *b*-modification.

Ethyl *b*-amide AdoCbl (3) on the other hand induces the expected intensity changes at all ten cleavage sites showing that the presence of the apical ligand in (3) overtakes any aberrance provoked by the introduced ethyl-group at the *b*-sidechain and allowing a correct switch (Figure 3B). Quantitative evaluation of the in-line probing titration experiments led to  $K_D$ -values of  $29 \pm 10 \mu\text{M}$  for 1, which is in the same order of magnitude as Vitamin B<sub>12</sub>, and  $38 \pm 12 \text{ nM}$  for 3 demonstrating again the high impact of the apical ligand for increasing ligand affinity (Table 1, for detailed evaluation, see Figure S16).<sup>[29]</sup> Interestingly, both (1) and (3) have a slightly elevated affinity towards the riboswitch compared to CNCbl and AdoCbl respectively implying that the ethyl group rather increases the van der Waals shape complementarity. The hydrogen bonds can most probably still be formed and if weakened, the additional hydrophobic contribution is more determinant.

The second modification at sidechain *b* comprises a carboxylate. The correspondent CNCbl derivative, *b*-acid CNCbl, was previously shown to induce an altered reorganization of the *btuB* riboswitch and to lower its affinity by a factor of ten compared to Vitamin B<sub>12</sub>.<sup>[15]</sup> Titration experiments performed with *b*-acid AdoCbl (5) now showed, that 5 is able to correctly switch the *btuB* riboswitch with only site 2b not being influenced (Figure S.13). The affinity of *b*-acid AdoCbl to the RNA ( $K_D = 470 \pm 157 \text{ nM}$ ) is about five times lower than that observed for AdoCbl ( $K_D = 89 \pm 6 \text{ nM}$ )<sup>[8]</sup> but is still around thousand fold higher as observed for Vitamin B<sub>12</sub> (Table 2). This observation correlates with the results from the ethylamide-derivatives 1 and 3 and fortifies the assumption that the apical adenosyl-ligand can overtake any aberrations induced by side-chain *b*-modifications.

### ***Modifications at Sidechain e Are Better Tolerated by the btuB Riboswitch***

The role of sidechain *e* for riboswitch recognition and refolding is not as clear as for sidechain *b* since its involvement in ligand/RNA-interaction is not consistent in the available crystal structures. Although this sidechain is always protruding towards the P11 region of the riboswitch, in the crystal structure of the *Symbiobacterium thermophilum* (*Sth*) riboswitch the sidechain *e* N–H acts as donor in a hydrogen bond with an oxygen belonging to G109,<sup>[14]</sup> while in the structure of the *Thermoanaerobacter tengcongensis* (*Tte*) riboswitch the *e*-amide group is

**Table 1.** Log  $K_s$  and  $K_D$  values for the binding of ethyl *b*-amide CNCbl (1), ethyl *b*-amide AdoCbl (3), dimethyl *e*-amide CNCbl (2) and dimethyl *e*-amide AdoCbl (4) to the *btuB* riboswitch. The values derived from each cleavage site are listed, as well as the average affinities and the corresponding  $K_D$  of these four new  $B_{12}$  derivatives to the riboswitch. Results obtained for CNCbl and AdoCbl are also given for comparison and do not contain values for site 6b. The values for each site are the weighted mean of three independent experiments and all errors given correspond to one standard deviation.

| Site    | CNCbl <sup>[8]</sup> | AdoCbl <sup>[8]</sup> | ethyl <i>b</i> -amide CNCbl (1) | ethyl <i>b</i> -amide AdoCbl (3) | dimethyl <i>e</i> -amide CNCbl (2) | dimethyl <i>e</i> -amide AdoCbl (4) |
|---------|----------------------|-----------------------|---------------------------------|----------------------------------|------------------------------------|-------------------------------------|
| 1       | 4.09 ± 0.02          | 7.11 ± 0.05           | - [a]                           | 7.40 ± 0.11                      | - [a]                              | 7.08 ± 0.09                         |
| 2       | 3.39 ± 0.22          | 7.06 ± 0.05           | 4.24 ± 0.14 [b]                 | 6.81 ± 0.25 [d]                  | 3.61 ± 0.01 [b]                    | 6.91 ± 0.19 [b]                     |
| 2b      | 3.52 ± 0.29          | 7.13 ± 0.10           | 4.69 ± 0.18 [b][c]              | 7.47 ± 0.03                      | -                                  | 7.12 ± 0.05                         |
| 3       | 3.45 ± 0.08          | 7.04 ± 0.05           | 4.20 ± 0.13 [c]                 | 7.43 ± 0.13 [b]                  | -                                  | 6.90 ± 0.10                         |
| 4       | 3.47 ± 0.18          | 7.06 ± 0.03           | -                               | 7.26 ± 0.27                      | -                                  | 6.97 ± 0.12                         |
| 5       | 3.21 ± 0.48          | 6.87 ± 0.40           | -                               | 6.65 ± 0.29 [d]                  | -                                  | 6.90 ± 0.17 [d]                     |
| 6       | 3.37 ± 0.31          | 7.01 ± 0.03           | 4.81 ± 0.08 [b]                 | 6.43 ± 0.17 [b]                  | 3.68 ± 0.02 [b]                    | 6.60 ± 0.33 [b]                     |
| 6b      | -                    | -                     | - [a]                           | 7.20 ± 0.31 [d]                  | 3.78 ± 0.20 [b]                    | 7.47 ± 0.09 [d]                     |
| 7       | 3.40 ± 0.50          | 7.00 ± 0.07           | 4.31 ± 0.15 [b]                 | - [a]                            | 3.67 ± 0.35 [b]                    | -                                   |
| 8       | 3.63 ± 0.11          | 6.52 ± 1.63           | - [a]                           | 6.85 ± 0.25 [b]                  | - [a]                              | 7.16 ± 0.12                         |
| average | 3.50 ± 0.20          | 7.05 ± 0.03           | 4.54 ± 0.14                     | 7.42 ± 0.14                      | 3.63 ± 0.04                        | 7.11 ± 0.07                         |
| $K_D$   | 314 ± 141 μM         | 89 ± 6 nM             | 29 ± 10 μM                      | 38 ± 12 nM                       | 234 ± 20 μM                        | 78 ± 12 nM                          |

[a] A change is visible, but data could not be fitted [b] Average from two titrations only [c] Trend opposite to the one expected are shown in grey [d] Value from one titration.

**Table 2.** log  $K_s$  and  $K_D$  values for the binding of the AdoCbl acid-derivatives *b*-acid AdoCbl (5) and *e*-acid AdoCbl (6). The values derived from each cleavage site are listed, as well as the average affinities and the corresponding  $K_D$  values. Results obtained for the corresponding CNCbl-derivatives are given for comparison. Results obtained for CNCbl and AdoCbl are also given for comparison and do not contain values for site 6b. The values for each site are the weighted mean of three independent experiments and all errors given correspond to one standard deviation.

| Site    | CNCbl <sup>[8]</sup> | AdoCbl <sup>[8]</sup> | <i>b</i> -acid CNCbl <sup>[15]</sup> | <i>b</i> -acid AdoCbl (5) | <i>e</i> -acid CNCbl <sup>[15]</sup> | <i>e</i> -acid AdoCbl (6) |
|---------|----------------------|-----------------------|--------------------------------------|---------------------------|--------------------------------------|---------------------------|
| 1       | 4.09 ± 0.02          | 7.11 ± 0.05           | 2.50 ± 0.04                          | 6.43 ± 0.04               | 3.56 ± 0.04                          | 6.59 ± 0.18               |
| 2       | 3.39 ± 0.22          | 7.06 ± 0.05           | -                                    | 6.10 ± 0.15 [b]           | -                                    | - [a]                     |
| 2b      | 3.52 ± 0.29          | 7.13 ± 0.10           | -                                    | -                         | -                                    | 6.65 ± 0.12               |
| 3       | 3.45 ± 0.08          | 7.04 ± 0.05           | -                                    | 6.64 ± 0.13               | -                                    | 6.66 ± 0.10               |
| 4       | 3.47 ± 0.18          | 7.06 ± 0.03           | -                                    | 6.51 ± 0.08 [b]           | -                                    | 7.07 ± 0.15               |
| 5       | 3.21 ± 0.48          | 6.87 ± 0.40           | -                                    | 5.54 ± 0.12 [b]           | -                                    | -                         |
| 6       | 3.37 ± 0.31          | 7.01 ± 0.03           | -                                    | 5.66 ± 0.26 [b]           | -                                    | - [a]                     |
| 6b      | -                    | -                     | -                                    | 5.48 ± 0.14 [b]           | -                                    | 7.20 ± 0.22 [c]           |
| 7       | 3.40 ± 0.50          | 7.00 ± 0.07           | -                                    | - [a]                     | -                                    | -                         |
| 8       | 3.63 ± 0.11          | 6.52 ± 1.63           | 2.71 ± 0.54                          | 6.41 ± 0.08 [b]           | 3.60 ± 0.04                          | 7.13 ± 0.17 [c]           |
| average | 3.50 ± 0.20          | 7.05 ± 0.03           | 2.50 ± 0.11                          | 6.33 ± 0.14               | 3.58 ± 0.02                          | 6.81 ± 0.11               |
| $K_D$   | 314 ± 141 μM         | 89 ± 6 nM             | 3.16 ± 0.80 mM                       | 470 ± 157 nM              | 263 ± 12 μM                          | 156 ± 39 nM               |

[a] A change is visible, but the data could not be fitted [b] Average from two titrations only [c] Value from one titration.

too far from the surrounding atoms to be involved in this type of interaction.<sup>[13]</sup> Therefore, the role of the *e*-sidechain for riboswitch recognition and/or refolding seems to be, at the first sight, less uniform than the involvement of the *b*- or the *c*-sidechains.

In-line probing titration experiments showed that the insertion of two methyl groups at the amide sidechain *e* to abolish any H-bonding interaction at this site leads to an incomplete switch of the *btuB* riboswitch. After addition of (2) only about half of the sites show the expected trend in cleavage intensity, while sites 2b, 3, 4 and 5 remain unaffected (Figure S.14 A, red versus grey sites). As found for *b*-amide CNCbl

(1) the unaffected sites are again located in the P6-extension (Figure S.14 A, grey sites). The overall affinity of 2 to the riboswitch is very similar to Vitamin  $B_{12}$  (Table 1).

The essential role of the adenosyl apical ligand for the affinity to the *btuB* riboswitch is evident also for this pair of  $B_{12}$  derivatives since dimethyl *e*-amide AdoCbl (4) shows a very high affinity to the RNA ( $K_D = 78 \pm 12$  nM) which is comparable to the natural ligand AdoCbl. All known cleavage sites of the riboswitch except site 7 are affected by the presence of dimethyl *e*-amide AdoCbl (Figure S.14B). Again, these results point to the ability of the apical adenosyl ligand to minimize any aberrations induced by sidechain *e*-modifications. Thus, the



complete inability of **4** to undergo H-bonding interaction through sidechain *e* does neither affect its affinity to the riboswitch nor allow a complete structural rearrangement thereof. It is therefore very likely that the binding scheme of the *btuB* riboswitch is similar to the one of the *Tte* riboswitch<sup>[13]</sup> not involving sidechain *e* in the H-bonding network.

Titration experiments performed with *e*-acid AdoCbl (**6**) showed, that also this compound can induce a nearly complete switch of the *btuB* riboswitch (Figure S.15) with high affinity ( $K_D = 156 \pm 39$  nM, Table 2). It should be noted that in an earlier study using Vitamin B<sub>12</sub> derivatives,<sup>[15]</sup> introduction of a negatively charged moiety at sidechain *e* was found to have a smaller impact than for sidechain *b* retaining its binding affinity in the same magnitude as Vitamin B<sub>12</sub> ( $K_D = 253 \pm 12$  μM). The high affinities of both, *e*-acid CNCbl and **6** demonstrate that the electrostatic repulsion between the carboxylate and the phosphates of nearby nucleotides is not destabilizing the B<sub>12</sub>-RNA interaction and further support the hypothesis that the *e*-amide group is not directly involved in strong hydrogen bonds necessary for recognition and structural change. On the other hand, we here demonstrated that introduction of alkyl groups on the amidic nitrogen generally leads to a slightly increased affinity for all compounds tested (**1** to **4**), confirming the importance of the van der Waals shape complementarity for the B<sub>12</sub>-RNA interaction, already noticed in the crystal structures solved.<sup>[13,14]</sup>

## Conclusions

The scope of this study is to characterize and understand the involvement of the two β-sidechains *b* and *e* of cobalamin in their interaction with the *btuB* riboswitch of *E. coli*. We have synthesized six different B<sub>12</sub> derivatives modified with either a substituted amide or a carboxylic acid at the indicated sidechains and carrying either a cyano- or adenosyl-ligand making them vitamin B<sub>12</sub> or coenzyme B<sub>12</sub> derivatives respectively. The six derivatives were synthesized with yields of around 30%, which is primarily due to the formation of stable intermediates.

In-line probing experiments with the *btuB* riboswitch of *E. coli* allowed us to monitor the influence of these modifications for the B<sub>12</sub>-riboswitch interaction. For the vitamin B<sub>12</sub>-derivatives, we found that modifications on the sidechain *b* led to notable changes. The conversion of the natural primary *b*-amide into a secondary amide group, leads to a slight increase in affinity, however, the structural rearrangement of the riboswitch is very much disturbed. The same holds true for the *b*-acid derivative studied earlier, where the affinity is decreased dramatically due to electrostatic repulsion and/or to the disruption of relevant contacts with the RNA. As anticipated by the crystal structures of B<sub>12</sub> riboswitches published so-far, the *b*-sidechain has a key role in the stabilization of the ligand-RNA interaction especially in the case of so-called small B<sub>12</sub> derivatives like vitamin B<sub>12</sub>, which in principle can bind to the *btuB* riboswitch and induce a correct reorganization thereof. Similar chemical modifications on sidechain *e*, whose involvement in the interaction varies with the individual riboswitch,

did not influence the affinity significantly compared to vitamin B<sub>12</sub>. However, also in this case, we observed an incomplete reorganization of the riboswitch. Sidechain *e* better tolerates chemical modifications and seems not to be involved in crucial hydrogen bonds with the RNA. Therefore, sidechain *e* could potentially be further modified if specific functionalities need to be inserted in the B<sub>12</sub> derivative.

Our work fortifies the determinant role of the apical adenosyl ligand not only for a high affinity binding to the riboswitch but also for restoring the correct structure of the riboswitch despite the presence of unfavorable modifications. We have observed and described for the first time that for all modifications studied here, even the ones at site *b*, the switch was restored to nearly full extent once the adenosyl ligand was present. Our investigations reaffirm the previously established notion that the introduction of negative charges or the alteration of donor sidechains to acceptor is unfavorable for binding.<sup>[15]</sup> Most importantly, the riboswitch exhibits a much greater tolerance towards modifications on sidechain *e* compared to sidechain *b*, suggesting sidechain *e* as a promising locus for the strategical design of binders aimed at modulating the regulatory mechanism of the *btuB* riboswitch. Furthermore, the attachment of alkyl groups at sidechain *b* presents a possibility to enhance the binding affinity, potentially mitigating the effects of other introduced modifications at sidechain *e*. These insights aid the development of tailored binders of the *btuB* riboswitch with potentially biotechnological applications.

## Supporting Information Summary

The Supporting information including a full experimental description of the syntheses, the characterization of the compounds and detailed information of the biochemical assays is available free of charge on the Publications website. Included are also relevant NMR- and UV/Vis spectra, HPLC-traces, further in-line probing gels and an example of their evaluation. The authors have cited additional references within the Supporting information.<sup>[28–32]</sup>

## Acknowledgements

Financial support by the European Research Council (ERC Starting grant 2010 to RKOS), the Swiss National Science Foundation (Projects 200020\_165868 and 200020\_192153) and the University of Zurich is gratefully acknowledged. We thank the former undergraduate students Thomas Nipkov and Sara Da Ros for synthesizing a batch of (**1**) and (**5**) respectively. Open Access funding provided by Universität Zürich.

## Conflict of Interests

The authors declare no conflict of interest.

## Data Availability Statement

The data that support the findings of this study are available in the supplementary material of this article.

**Keywords:** RNA · Riboswitch · Footprinting · Vitamin B<sub>12</sub> derivatives

- [1] A. Nahvi, N. Sudarsan, M. S. Ebert, X. Zou, K. L. Brown, R. R. Breaker, *Chem. Biol.* **2002**, *9*, 1043.
- [2] a) A. S. Mironov, I. Gusarov, R. Rafikov, E. Lopez Lubov, K. Shatalin, R. A. Krenova, D. A. Perumov, E. Nudler, *Cell* **2002**, *111*, 747; b) N. Sudarsan, J. E. Barrick, R. R. Breaker, *RNA (New York, N. Y.)* **2003**, *9*, 644; c) W. Winkler, A. Nahvi, R. R. Breaker, *Nature* **2002**, *419*, 952.
- [3] a) J. K. Soukup, G. A. Soukup, *Curr. Opin. Struct. Biol.* **2004**, *14*, 344; b) W. C. Winkler, R. R. Breaker, *ChemBioChem: Eur. J. Chem. Biol.* **2003**, *4*, 1024; c) T. Kubodera, M. Watanabe, K. Yoshiuchi, N. Yamashita, A. Nishimura, S. Nakai, K. Gomi, H. Hanamoto, *FEBS letters* **2003**, *555*, 516; d) W. C. Winkler, A. Nahvi, A. Roth, J. A. Collins, R. R. Breaker, *Nature* **2004**, *428*, 281; e) E. Loh, O. Dussurget, J. Gripenland, K. Vaitkevicius, T. Tiensuu, P. Mandin, F. Repoila, C. Buchrieser, P. Cossart, J. Johansson, *Cell* **2009**, *139*, 770; f) L. Bastet, A. Dubé, E. Massé, D. A. Lafontaine, *Mol. Microbiol.* **2011**, *80*, 1148.
- [4] M. Mandal, R. R. Breaker, *Nat. Rev. Mol. Cell Biol.* **2004**, *5*, 451.
- [5] W. C. Winkler, R. R. Breaker, *Annu. Rev. Microbiol.* **2005**, *5*, 451.
- [6] a) P. R. Reynolds, G. P. Mottur, C. Bradbeer, *J. Biol. Chem.* **1980**, *255*, 4313; b) A. Gudmundsdottir, C. Bradbeer, R. J. Kadner, *J. Biol. Chem.* **1988**, *263*, 14224; c) D. P. Chimento, A. K. Mohanty, R. J. Kadner, M. C. Wiener, *Nat. Struct. Biol.* **2003**, *10*, 394; d) X. Nou, R. J. Kadner, *PNAS* **2000**, *97*, 7190.
- [7] a) R. K. Montange, E. Mondragón, D. van Tyne, A. D. Garst, P. Ceres, R. T. Batey, *J. Mol. Biol.* **2010**, *396*, 761; b) A. Serganov, Y.-R. Yuan, O. Pikovskaya, A. Polonskaia, L. Malinina, A. T. Phan, C. Hobartner, R. Micura, R. R. Breaker, D. J. Patel, *Chem. Biol.* **2004**, *11*, 1729.
- [8] S. Gallo, M. Oberhuber, R. K. O. Sigel, B. Kräutler, *ChemBioChem: Eur. J. Chem. Biol.* **2008**, *9*, 1408.
- [9] K. J. Kennedy, F. J. Widner, O. M. Sokolovskaya, L. V. Innocent, R. R. Procknow, K. C. Mok, M. E. Taga, *mBIO* **2022**, *13*, e0112122.
- [10] C. W. Chan, A. Mondragón, *Nucleic Acids Res.* **2020**, *48*, 7569.
- [11] J. T. Polaski, S. M. Webster, J. E. Johnson, R. T. Batey, *J. Biol. Chem.* **2017**, *292*, 11650.
- [12] a) H. M. Marques, *J. Inorg. Biochem.* **2023**, *242*, 112154; b) P. D. Mestizo, C. Brenig, R. Stephan, F. Zelder, F. Muchaamba, *LWT* **2024**, *191*, 115641.
- [13] J. E. Johnson, F. E. Reyes, J. T. Polaski, R. T. Batey, *Nature* **2012**, *492*, 133.
- [14] A. Peselis, A. Serganov, *Nat. Struct. Mol. Biol.* **2012**, *19*, 1182.
- [15] S. Gallo, S. Mundwiler, R. Alberto, R. K. O. Sigel, *Chem. Comm. (Cambridge, England)* **2011**, *47*, 403.
- [16] P. K. Choudhary, S. Gallo, R. K. O. Sigel, *Methods Mol. Biol.* **2014**, *1086*, 143.
- [17] B. Spingler, S. Mundwiler, P. Ruiz-Sánchez, D. R. van Staveren, R. Alberto, *Eur. J. Inorg. Chem.* **2007**, *2007*, 2641.
- [18] P. M. Pathare, D. S. Wilbur, S. Heusser, E. V. Quadros, P. McLoughlin, A. C. Morgan, *Bioconjug. Chem.* **1996**, *7*, 217.
- [19] K. L. Brown, S. C. Cheng, H. M. Marques, *Inorg. Chem.* **1995**, *34*, 3038.
- [20] D. Doddrell, A. Allerhand, *Proc. Nat. Acad. Sci. USA* **1971**, *68*, 1083.
- [21] M. F. Summers, L. G. Marzilli, A. Bax, *J. Am. Chem. Soc.* **1986**, *108*, 4285.
- [22] P. K. Choudhary, S. Gallo, R. K. O. Sigel, *Front. Chem.* **2017**, *5*, 1.
- [23] B. Kräutler, *Met. Ions Life Sci.* **2009**, *6*, 1.
- [24] F. Wagner, K. Bernhauer, *Ann. N. Y. Acad. Sci.* **1964**, *112*, 580.
- [25] E. E. Regulska, R. R. Breaker, *Methods Mol. Biol.* **2008**, *419*, 453.
- [26] P. K. Choudhary, *PhD Thesis*, University of Zurich, Switzerland, **2013**.
- [27] a) A. Nahvi, J. E. Barrick, R. R. Breaker, *Nucleic Acids Research* **2004**, *32*, 143; b) A. G. Vitreschak, D. A. Rodionov, A. A. Mironov, M. S. Gelfand, *RNA* **2003**, *9*, 1084.
- [28] M. Nagaraju, G. Narahari Sastry, *J. Mol. Model.* **2011**, *17*, 1801.
- [29] R. K. O. Sigel, E. Freisinger, B. Lippert, *J. Biol. Inorg. Chem.* **2000**, *5*, 287.
- [30] M. J. Robins, S. F. Hansske, S. F. Wnuk, T. Kanai, *Can. J. Chem.* **1991**, *69*, 1468.
- [31] K. L. Brown, S. Cheng, H. M. Marques, *Polyhedron* **1998**, *17*, 2213.
- [32] S. Gallo, M. Furler, R. K. O. Sigel, *Chimia* **2005**, *59*, 812.
- [33] a) *End labeling procedures*. (Ed: E. Hilario), Humana Press, Totowa, NJ **2002**; b) E. Hilario, *Molecular biotechnology* **2004**, *28*, 77.

Manuscript received: May 7, 2024

Accepted manuscript online: June 23, 2024

Version of record online: August 13, 2024